Matrix print actuator for dot band printer

by J. L. Zable E. F. Helinski

The design selection of an impact matrix print actuator is described, along with its method of design and optimization. The dot band printer concept is discussed in conjunction with operational requirements for the hammer; these requirements, and methods of meeting them, are presented.

Introduction

Impact matrix printing typically has been limited to serial printer and relatively low-speed line printer configurations [1]. Among the advantages of matrix printing are font flexibility, graphics, and all-points-addressable capability. The apparent disadvantage of impact matrix printing seems to be its speed or throughput limitation; this is basically caused by the packaging limitations of the entire hammer unit and, to a limited extent, by the time required to move paper into position behind the printhead (the paper increment time).

This apparent throughput disadvantage of matrix printing could be overcome by selecting an appropriate low-cost line-matrix printer configuration. One such line-matrix printer configuration, called a dot band printer (Figure 1), is the IBM 4234 Printer. In this printer, a print band containing equally spaced flexible "fingers" in a chevron configuration moves continuously in front of a

[®]Copyright 1989 by International Business Machines Corporation. Copying in printed form for private use is permitted without payment of royalty provided that (1) each reproduction is done without alteration and (2) the *Journal* reference and IBM copyright notice are included on the first page. The title and abstract, but no other portions, of this paper may be copied or distributed royalty free without further permission by computer-based and other information-service systems. Permission to *republish* any other portion of this paper must be obtained from the Editor.

stationary bank of hammers [2]. Each finger or chevron contains an anvil that is always in contact with one of the hammer faces. On the other side of the anvil is a protruding "dot" which faces the ribbon and paper. When a dot is to be printed, the hammer is actuated, propelling the chevron and its protruding dot into the ribbon and paper. The paper, which is on tractors, is supported by a stationary rigid platen. The pitch of the chevrons is somewhat greater than the pitch of the hammers in order to avoid nipping between the edge of the hammer face and the anvil.

A line of printed dots is completed (print cycle) when the band moves a distance of one chevron pitch past the stationary hammer bank. During this time the hammers are being fired in accordance with the desired dot pattern to be printed. The paper is then advanced to the next row of dots to be printed. This cycle is repeated until a character row is completed. At this time, the paper is advanced to the top of the next character row to be printed.

Aside from the paper-movement time, the throughput of this printer is directly related to the repetition rate of the hammers. This is the rate at which the hammer can reliably strike the band-ribbon-paper for successive dots. Additionally, the width of the hammer, or hammer pitch, directly influences the anvil pitch, which is inversely related to throughput. However, because of cost-performance trade-offs, a hammer pitch of 0.300 inches was selected. In other words, each hammer can print three characters (ten characters per inch is the standard character spacing).

Hammer unit requirements

The key component of this printer, as with any impact line printer, is the hammer unit. Using a dot band

609

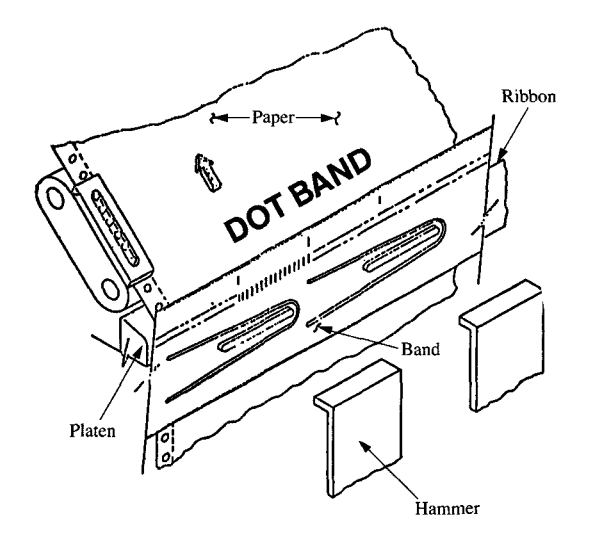


Figure 1
Schematic of dot band printer.

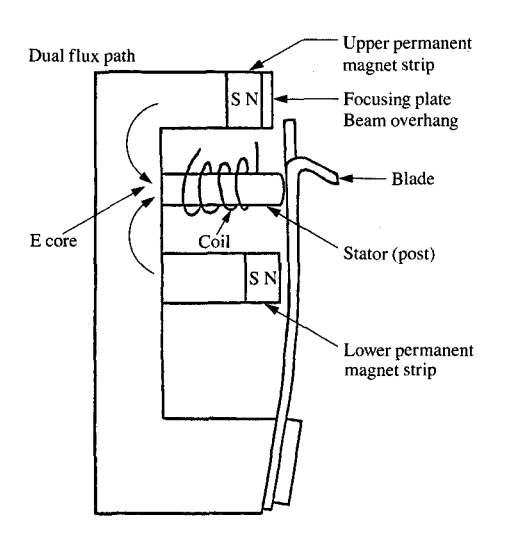


Figure 2

Cross section of hammer and magnet assembly.

approach in a low-cost, line-matrix configuration, however, produced unique and conflicting design requirements. Aside from the usual matrix-hammer requirements (reliable printing on one- to six-part forms, good print quality, etc.), this dot band printer required an extremely low-cost hammer unit with relatively high performance. Each individual hammer had to have the ability to strike a chevron uniformly over the entire width of the hammer face without any interaction between adjacent hammer positions, to produce good print contrast over a width of three character positions, and to function reliably over the tolerance range of the entire hammer unit. The basic performance objectives were the following:

- An 0.0011-s cycle time with a 0.020-in. stroke, or travel
- An impact force on one-part through six-part forms that produces good print contrast and long ribbon life.
- A flight-time variation of $\pm 10\%$ of cycle time.

Additionally, those performance parameters had to be met over a broad range of operating conditions:

- A stroke variation that tolerates all manufacturing variations as well as expected wear throughout the life of the unit.
- All expected power-supply voltage variations.
- Worst-case temperature and humidity variations.
- Impact over the entire blade length.
- Printing on one-part through six-part forms.
- Assembly variations.
- Various worst-case print patterns developed to induce mechanical and magnetic disturbances.

In addition to these performance requirements, high reliability had to be maintained.

Design

• Overall design concept

A variety of hammer technologies are available for matrix printing. However, the two predominant technologies [1] are the work-magnet and the stored-energy mechanisms. The stored-energy hammer relies upon magnetic release of a cocked spring containing the hammer. This technology [3], which is found in the IBM 2213 printers, has the advantage of higher efficiency and higher potential speed. The actuator cycle time of the 2213, for example, is 0.0015 s for a 0.020-in. stroke. In the work-magnet technology, a pivot-mounted hammer is rotated by electromagnetic force during the print cycle to impact the paper-ribbon-platen combination to accomplish printing. The advantage of this technology, which is found in the IBM 5225 printers, is flight-time stability.

The stored-energy hammer technology was chosen because the speed requirements were deemed a greater challenge to achieve than the flight-time-variation requirements. The particular approach that was taken was an "E"-core configuration [3] (Figure 2), because of its potential for high performance and low cost.

Briefly, the mode of operation for the hammer unit is that the beam part of the hammer is cocked, or pulled back, by the forces provided by the permanent magnets on the upper and lower legs of the E-core. The upper part of the beam is thus subjected to force and pulled against the center leg or post of the E-core. In this cocked position, the forces from the permanent magnets create stored elastic energy in the beam.

For actuation, current is applied to the coil mounted on the post, or center leg, of the E-core. This creates a magnetic flux opposite to that created by the permanent magnets. Thus, the resultant flux, or holding force, is reduced to almost zero, and the beam is released. The blade, or impactor, flies forward, striking the paper. After impact, the current to the coil is turned off, and the permanent magnets again attract the beam to the cocked position. Excellent performance is achieved due to the high acceleration during the early part of the cycle when the cocked beam produces its maximum force.

The fundamental design philosophy of this hammer unit, or actuator, was to meet the performance objectives at an absolute minimum cost. The low-cost objective dictated the use of a minimum number of simple, readily manufacturable parts. Common parts would be shared by individual actuator positions wherever possible. Some examples of this are shown in **Figure 3**; the hammer block assembly incorporates a common E-core frame, magnets, and a focusing plate.

The armature, impactor, suspension, and spring function are all incorporated in a single part, the clamped, cantilevered beam which is attracted to the stator (post) near its unclamped end. The upper part of the unclamped portion functions as an armature, the formed section at the upper end acts as an impactor, and the elastic deflection characteristics supply both suspension and a spring function for the beam. Since this is a stored-energy actuator, the magnetic energy is converted to potential energy, which is stored when the cantilevered beam is cocked. The beam is fabricated from AISI 8620 steel and combines satisfactory magnetic characteristics with an excellent endurance limit. Because the beam armatures must function independently, the beam assembly was manufactured as a "comb," so that one part could serve multiple actuator positions.

The coil and adjustable stator (post) were the only pieces which remained discrete, resulting in a minimum number of parts.

• Procedure for selecting approximate beam geometry

The hammer beam performs multiple functions. It must store sufficient energy to print. It must have sufficient

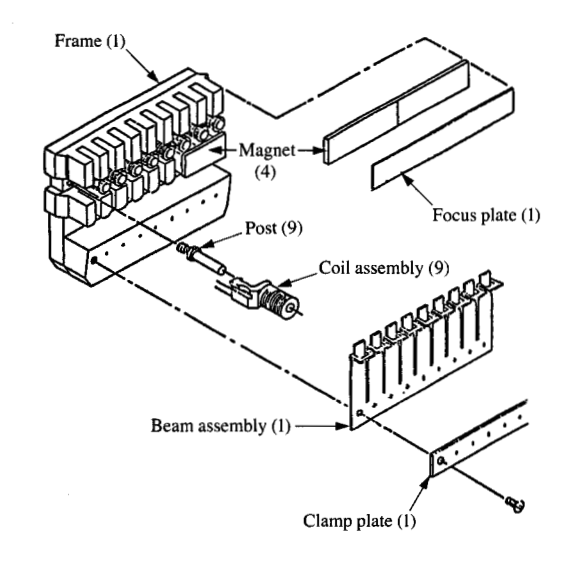


Figure 3 Hammer block assembly.

cross-sectional area to efficiently complete the magnetic circuit. It must have sufficient strength so that fatigue failures do not occur, and it must have sufficient torsional rigidity to provide good print quality for all three print positions covered by the hammer (beam blade). The beam must also provide adequate stroke travel without significant degradation of print force. From these requirements, various mathematical relationships can be developed.

Figure 4 shows three curves. Curve A is the magnetic force acting on the beam versus its displacement from its contact position on the post. Curve B is the negative of the potential spring force in the beam. The area under this curve is the maximum potential energy in the beam that could be converted to kinetic energy. Curve C is the resultant spring force actually obtained, since complete buck-out of Curve A by the coil current cannot occur. Thus, the area under Curve C is the actual energy E_0 available for printing.

From Figure 4 and Figure 5, D is the stroke distance over which the beam blade would travel if unimpeded, αD is the portion of D actually traversed before impact, and F_0 is the peak spring force in the beam. From Figure 4, we can derive

$$E_0 \approx \frac{1}{2} \alpha D \alpha F_0 \,.$$

Typically, for good printing with a 0.017-in. dot, this should be greater than 10 000 ergs. Thus,

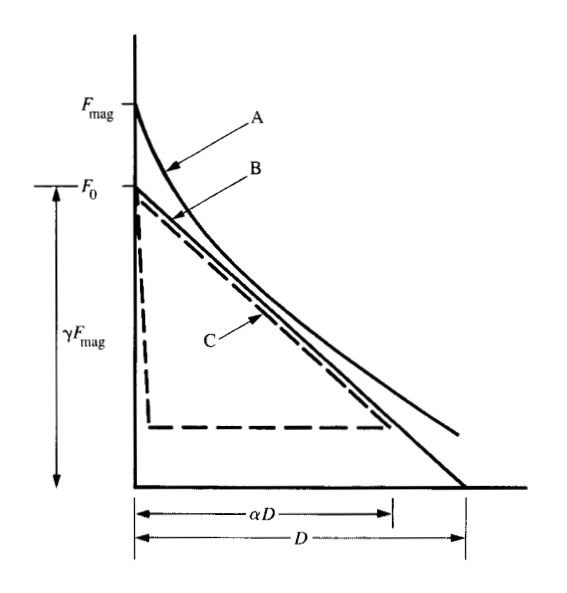


Figure 4

Magnetic and elastic deflection characteristics of beam.

$$(\alpha/2)D\alpha F_0 \ge 10\,000. \tag{1}$$

But, from beam theory [4],

$$F_0 = \frac{3EI}{\beta^3 \ell^3} D,\tag{2}$$

where E is the elastic modulus of the beam material, I is the area moment of inertia of the beam, ℓ is the length of the beam, and $\beta\ell$ is the distance from the fixed end of the beam to the position of the blade (Figure 6). The maximum static stress is

$$\nabla_{\max} = \frac{6F_0\beta\ell}{bh^2}.$$

This should be less than 70 000 psi; thus,

$$70\,000 > \frac{6F_0\beta\ell}{hh^2}.\tag{3}$$

The magnetic holding force should be such that it will always be great enough to attract the beam into the cocked position. Thus,

$$\frac{F_0}{F_{\text{mag}}} < \gamma.$$

Furthermore, the beam cross section should be large enough to allow the magnetic holding force $F_{\rm mag}$ to be realized. Thus [5],

$$F_{\rm mag} = 2B^2bh$$

and

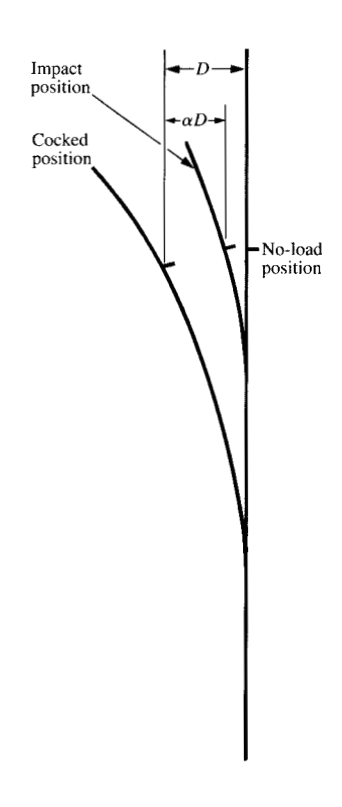
$$\frac{F_0}{2B^2bh} < \gamma, \text{ or } \frac{E\alpha D}{8B^2\beta^3\gamma\alpha} \left(\frac{h}{\ell}\right)^3 < h, \tag{4}$$

where B is the flux density for the beam material. The torsional rigidity requirement is such that there is 50 percent less impact force when the extreme edge of the blade strikes the paper first. This establishes a relationship between the energy that can remain to twist the beam, as opposed to that which goes into compressing the paper (printing). The relationship

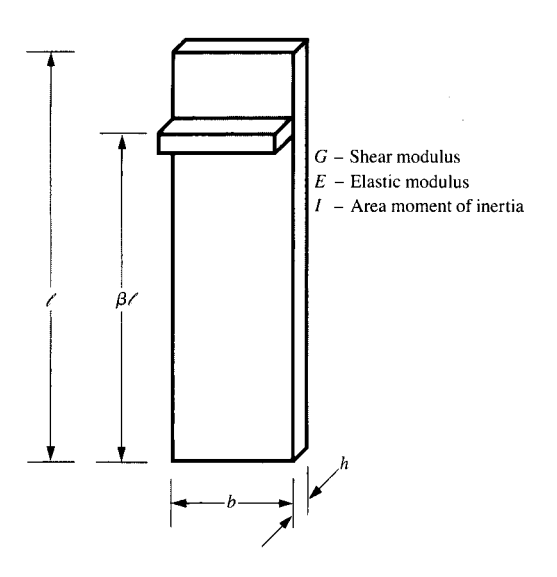
$$k_{\rm T} > k_{\rm p} \, \frac{b^2}{4} \left(\frac{0.72}{0.28} \right)$$

is obtained, where $k_{\rm T}$ is the torsional spring rate of the beam and $k_{\rm p}$ is the spring rate of a six-part form. Thus [6],

$$\frac{Gbh^{3}}{3 \beta \ell} > k_{p} \frac{b^{2}}{4} \left(\frac{0.72}{0.28} \right). \tag{5}$$



Mechanical deflection of beam.



Flaure 6

Front view of beam

Finally, the flight time of the hammer, which is approximately one-fourth of the period of oscillation at the beam's natural frequency, is [7]

$$t_{\rm f} = \frac{\left[\frac{\pi}{2} - (1 - \alpha)\right]h}{1.875^2 \frac{Eg}{12e} \left[\left(\frac{h}{\ell}\right)^{4}\right]^{1/2}},\tag{6}$$

where E is the modulus of elasticity for the beam, g is a gravity constant, and e is the density of the beam material.

With Equations (1) through (6), we can now estimate the optimum beam dimensions. Since this is for a threeprint-position hammer design, the following rough parameters were assumed:

$$b = 0.26$$
,

$$\alpha = 0.7, \beta = 0.9, \gamma = 0.8,$$

 $k_{\rm p} = 500 \, \text{lb/in.},$

 $B = 16\,000$ gauss,

 $\alpha D = 0.020 \text{ in.}$

The curves of **Figure 7** are generated by the above equations and parameter values. The curves of the first and second quadrant establish the minimum h/ℓ required for sufficient print energy. As seen from quadrant 2, this

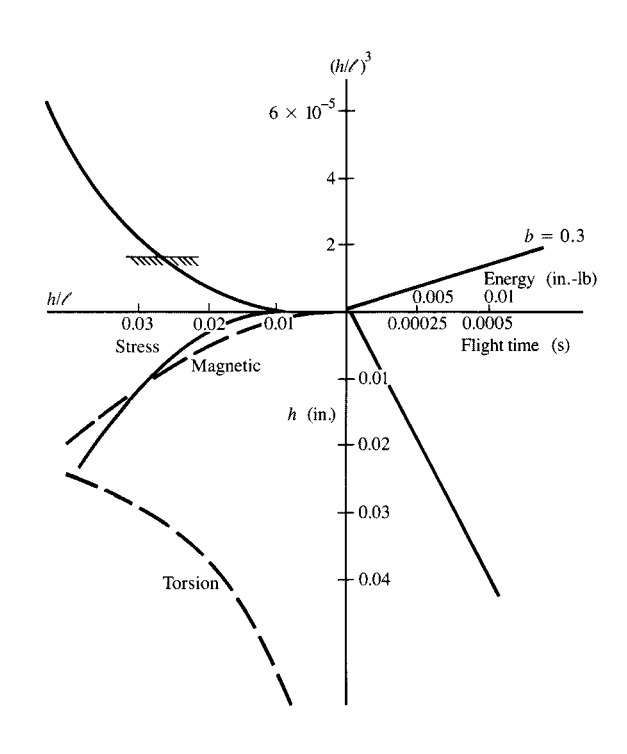


Figure 7

Design curves.

value must be greater than 0.024. Quadrant 3 contains the curves showing the limitations of stress, magnetic flux, and torsional rigidity. The torsional-rigidity requirement for this design is the most stringent. This leads to a beam thickness of approximately 0.032 in. and a beam length of approximately 1.5 in. As can be seen from quadrant 4, the flight time should be approximately $360~\mu s$. Thus, with a contact time of $150~\mu s$ and a return time typically equal to the sum of the flight time and the contact time, a total cycle time of approximately 1 ms is estimated for performance. Thus, these beam dimensions can be used as a start for beam geometry optimization.

• Mechanical optimization

The detailed design of this cantilevered beam and its relationship to the impactor are such that it is necessary to have a portion of the cantilevered beam extend beyond the impactor to ensure that secondary impacts do not occur during printing [8]. Thus, the impactor is located near the nodal point for the second mode of vibration. Similarly, the stator (post) is located opposite the impactor to ensure that settle-out of the beam is rapid and that the cycle time is not significantly related to the settle-out characteristics of the beam.

Therefore, we understood the mechanical significance of beam overhang; in addition, however, we recognized that the use of this overhang as one of the two primary flux paths would lead to an optimized mechanical and magnetic design point.

The beam could be tapered, making the upper, more critical end low in mass. This would maintain a high spring-rate-to-effective-mass ratio, while providing a cross-sectional area through the two magnetic flux paths that was minimal but sufficient to provide the necessary magnetic energy to retract the beam to a spring-loaded condition.

The flux paths are magnetically saturated by the permanent magnets. Because of this, consistent performance characteristics can be achieved which are relatively insensitive to minor variations in the characteristics of the permanent magnets, or to minor variations in gap distances between the beam and the permanent magnets.

In the design of the overhanging beam, it is desirable to provide just enough overhang to prevent secondary impacts. Minimizing the overhang mass results in the smallest effective mass at the impactor and leads to the attainment of the greatest operating repetition rate. This minimal overhang, however, is not inherently efficient in transferring magnetic flux from the upper permanent magnet (Figure 2) to the stator, because of the small amount of overlap between the magnet and the beam end. This deficiency was overcome by bonding a magnetically permeable (soft steel) focusing plate to the magnet. This improved flux path makes optimal use of the magnetic material and requires no additional beam mass or beam overlap. In addition, this modification does not require dynamically interleaved parts or close tolerances, making it consistent with cost objectives for the actuators.

The impact surfaces of both beam and stator (post) are the areas most subject to wear, and these are protected with hard chrome plate.

• Magnetic optimization

Magnetic optimization can be divided into two categories, optimization of the permanent magnet structure (least magnetic volume), and optimization of the electromagnetic circuit (high efficiency). The E-core configuration in Figure 2 describes two operational flux paths. This construction allows the use of rare-earth strip magnets, which are located as close as practicable to the working gap of the actuator. Also, the flux paths are short and simple, permitting the use of relatively thin magnets which contribute to both high efficiency and minimal use of material.

Locating permanent magnets close to the working gap minimizes flux leakage, allowing a larger percentage of the total magnetomotive force (MMF) to reach the working gap and thereby minimizing the magnetic material.

Similarly, an optimization of the electromagnetic circuit occurs when the reluctance of the magnetic path is minimized. Additionally, a large percentage of the flux that the coil produces should reach the working magnetic gap to cancel the permanent magnets' flux at the gap. This condition generally works best when the coil is centered over the working gap. However, since this was not practical for this design, locating the working gap near the end of the coil was a satisfactory compromise.

• Coil optimization

Coil optimization was done using substantially empirical techniques with general analytical guidelines.

It was empirically determined that a stator with a diameter of 0.125 in. would carry sufficient magnetic energy to attract the beam into a spring-loaded condition and store enough energy in the beam to cause satisfactory printing.

This left only the length-to-diameter ratio of the coil to be optimized. This ratio is used to determine the maximum coil length [9]; i.e.,

$$C = \frac{l}{(OD + ID)/2},$$

where l = coil length, OD = coil outside diameter, ID = coil inside diameter, and C = length-to-diameter ratio.

Values of C above 1.5 result in flux leakage, which increases sharply with increases in generated flux. It was experimentally verified that a value of C equal to 1.3 resulted in the best operational performance.

After the length and diameter of the coil were established, the remaining problem was to design the coil for a given operating voltage. This problem is simplified by realizing that the L/R time constant does not change for a fixed coil geometry and wire volume. Therefore, a large range of operating voltages may be used in conjunction with the appropriate choice of wire size.

To minimize I^2R losses in the switching devices and cables, it is advantageous to use maximum voltages, accounting for practical limitations. In this case, a maximum operating voltage of 32 V was established from the combined characteristics of the driver circuit and switching devices.

The wire size and number of turns were fine-tuned experimentally to this voltage, to obtain the proper number of ampere turns to optimally buck out the permanent magnetic flux in the working gap.

Electrical optimization

The current waveform shown in Figure 8 optimally matches the operating characteristics of both the

mechanical hardware and the electronic circuit. The current required to cancel the magnetic flux produced by the permanent magnet in the working gap is a function of time. That is, more ampere turns are required to cancel this flux in a short period of time, and fewer ampere turns are required for static conditions. This is due both to eddy-current effects and to the hysteresis characteristics of the core. Because of this, more current is required to achieve the initial buck-out, but after the permanent magnet's flux is canceled, a lower current will maintain a bucked-out state (Figure 8).

Also described in Figure 8 is the magnetic flux as a function of coil current. It can be seen that when the current is reduced from the 2.0-A peak to just under 1.0 A, the magnetic flux does not change significantly. This is because a nearly complete buck-out of the flux due to the permanent magnet takes place at a current level of 1.0 A under static conditions.

Testing

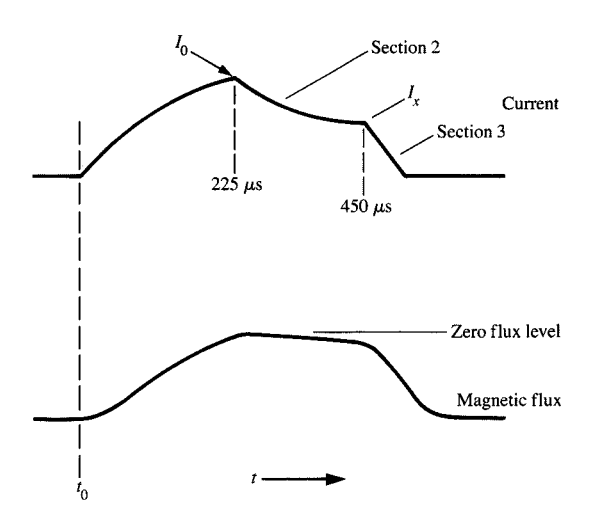
• Coil geometry and pulse

A number of coils were fabricated with variations in length, diameter, and wire size, with variations in the pulse applied to each. The output performance of the device was observed; uniformity of force over the entire expected stroke range was the most important characteristic. Table 1 describes the coil- and pulse-related parameters that produced the best force uniformity over the stroke range.

• Impact force versus stroke

There are many minor contributions that influence variations in impact force. One of the most predictable variables affecting impact force is the hammer stroke. Due to the nature of the stored-energy concept, the maximum energy and impact force occur at only one stroke, usually the nominal (0.015 in.). At strokes less than nominal, the energy stored in the cocked beam is not fully released. At strokes which are greater than nominal, some of the print energy is diverted into reverse deflection of the beam; this usually occurs after pulse turn-off. However, very significant variations are also caused by firing the hammer at a time when the hammers have not returned to their start condition, or are "unsettled." This is very frequently the case with matrix printers.

Figure 9 shows photographic traces of the print forces that result from successive firing at a repetition rate of 1.1 ms for three different strokes, 0.010, 0.015, and 0.020 inches. At this repetition rate, the hammer does not have time to settle between strokes; this unpredictable slight variation in hammer position can impart either more or less energy to the hammer on successive firings. The



Floure 8

Current and magnetic flux waveforms.

Table 1 Optimized electrical and physical parameters for the coil.

Coil outside diameter (in.)	0.271	
Coil inside diameter (in.)	0.136	
Coil length (in.)	0.310	
Wire size	#33	
Wire layers	9	
Wire turns	316	
Wire resistance units	3.8	
Voltage (V)	30	
Pulse (µs)	225	
Electrical energy (W-s)	0.008	

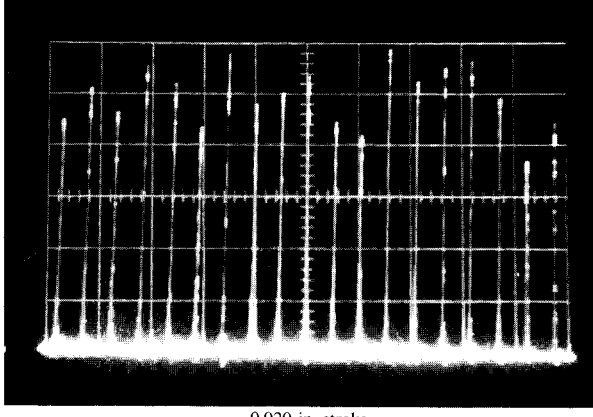
variations in print force shown in Figure 9, which are acceptable, thus result directly from the unsettled condition of the hammer.

• Impact force range versus impactor size

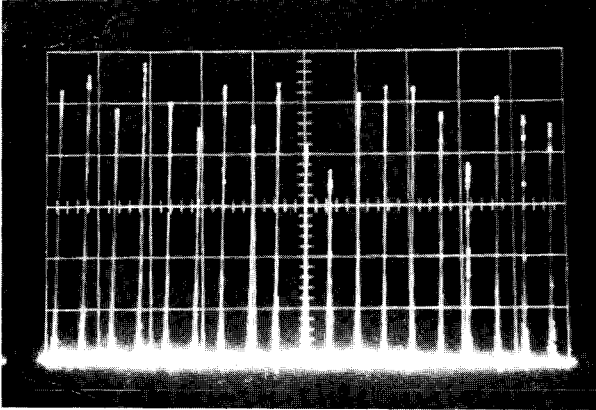
Figure 10 shows the experimental range of forces obtained while printing at various operating rates using a range of impactor sizes. The upper limit of allowable force is the force at which ribbon damage begins to occur; the lower limit is the force required for minimum acceptable print contrast. The actual forces produced were found to lie between the maximum and minimum allowable forces for the 0.016-in. impactor diameter.

• Results of all testing

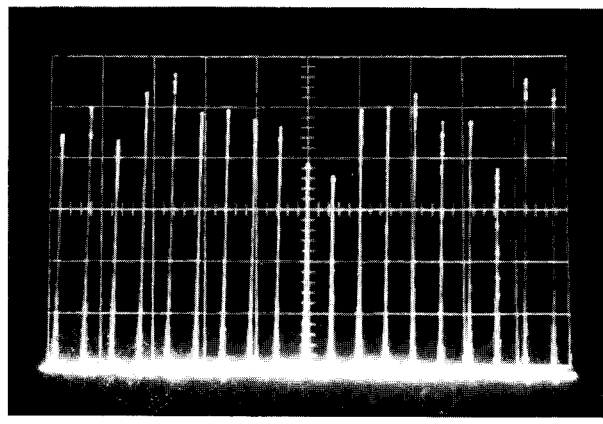
The testing described above verified that the hammer design had met all design objectives and requirements. In



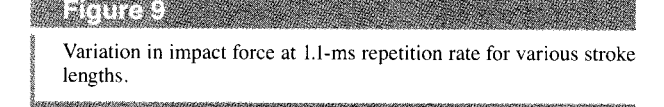




0.015-in. stroke



0.010-in. stroke



addition to the detailed testing, however, severe worstcase testing was also performed. This combined all the major worst-case conditions to determine whether the desired repetition rate was consistently attainable in a

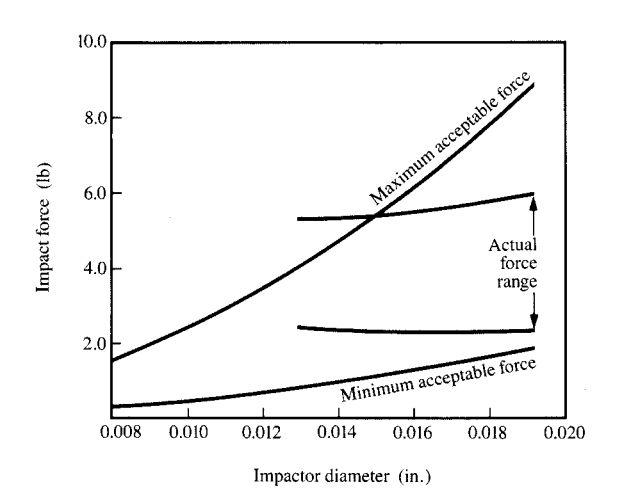


Figure 10

Range of acceptable impact force vs. impactor diameter.

general worst-case environment. Combinations of the worst-case values of voltage, magnetic gap, stroke, adjustment, beam geometry, and pulse width verified that a 1.1-ms repetition rate was in fact obtainable.

Summary

Uniqueness and practicability are the attributes which best describe the IBM 4234 dot band printer and its print actuator. Dot band printing provides new functional capabilities combined with high performance. The print actuator and its electronic coil driver operate at an efficiency of 13 percent, making it one of the most efficient commercially applied hammer designs known. The cost of the actuator is kept low as a result of its block design, which maximizes the use of commonly shared parts. The design is readily manufacturable and lends itself to robotic or manual assembly for further cost reduction.

The unit has undergone extensive worst-case simulated testing, helping it to meet a very high standard of reliable operation with excellent print quality.

The stored-energy actuator used in this printer has successfully met the challenge of providing high performance at low cost. This combination offers excellent value and state-of-the-art performance.

References

 T. Y. Nickel and F. J. Kania, "Printer Technology in IBM," IBM J. Res. Develop. 25, 755-765 (1981).

- H. C. Wang and R. E. McCurry, "Chapter 8: Other Impact Printing Technologies," *Output Hardcopy Devices*, Academic Press, Inc., San Diego, CA, March 1988.
- P. A. Brumbaugh, R. H. Harrington, S. F. Nemier, and T. C. Nielson, "Wire Matrix Print Head," U.S. Patent 3,672,482, 1972.
- 4. J. M. Gere and S. P. Timoshenko, *Mechanics of Materials*, 2nd Edition, Brooks/Cole Engineering, Monterey, CA, 1984.
- J. R. Reitz and F. J. Milford, Foundations of Electromagnetic Theory, 3rd Edition, Addison-Wesley Publishing Co., Reading, MA, 1984.
- E. J. Roark, Formulas for Stress and Strain, 4th Edition, McGraw-Hill Book Co., Inc., New York, 1965.
- E. Voleterra and E. C. Zachmanoglou, Dynamics of Vibrations, Charles Merrill Books Inc., Columbus, OH, 1965.
- J. G. Hamilton and J. E. Wallace, "Low Cost Hammer Unit," U.S. Patent 3,747,521, 1973.
- R. M. Bozorth, Ferromagnetism, 5th Edition, D. Van Nostrand Co., New York, 1951.
- H. C. Lee and J. L. Zable, "Chapter 6: Engraved Line Printing," *Output Hardcopy Devices*, Academic Press, Inc., San Diego, CA, March 1988.

Received August 27, 1986; revised manuscript received June 20, 1988; accepted for publication October 11, 1989

Jack L. Zable 1BM Data Systems Division, P.O. Box 6, Endicott, New York 13760. Dr. Zable is a senior technical staff member and is manager of the impact printer technology area in Endicott. He has been a member of the printer technology area since 1972, during which time he has developed mechanisms for both impact and nonimpact printers. Prior to this, he was a member of the mechanical analysis group in Endicott, where he performed theoretical and experimental analyses on a variety of high-speed mechanisms. In 1967 he was the recipient of an IBM Resident Study Scholarship, and received his Ph.D. in mechanical engineering from Purdue University, West Lafayette, Indiana, in 1969. Since 1971 he has also been an Adjunct Faculty Member in the Engineering Graduate School at the State University of New York at Binghamton. Dr. Zable is a member of the American Society of Mechanical Engineers, Pi Tau Sigma, and Sigma Xi.

Edward F. Helinski IBM Data Systems Division, P.O. Box 6, Endicott, New York 13760. Mr. Helinski received his A.S. in mechanical engineering from Pennsylvania State University, University Park, in 1963. After joining IBM in 1963, he worked on pneumatic logic technology until transferring to the printer technology area, where he is a senior engineer. Since 1972 Mr. Helinski has worked on both impact and nonimpact printer technologies; he has the distinction of being the highest-level inventor at the Endicott site.